Estimating Parameters for Rates of CO Poisoning and Recovery in a PEMFC Using a Pt/Ru-C Anode

by

Tochi Nwoga[*] and J. W. Van Zee[*, 1]
Department of Chemical Engineering
University of South Carolina
Columbia, SC 29208

[*]- ECS active member
[1] - Corresponding author: Phone: (803) 777-2285, Fax: (803) 777-8265, e-mail: vanzee@engr.sc.edu

1. REPORT DATE **01 JUN 2004**	2. REPORT TYPE **N/A**	3. DATES COVERED **-**	
4. TITLE AND SUBTITLE **Estimating Parameters for Rates of CO Poisoning and Recovery in a PEMFC Using a Pt/Ru-C Anode**		5a. CONTRACT NUMBER	
		5b. GRANT NUMBER	
		5c. PROGRAM ELEMENT NUMBER	
6. AUTHOR(S)		5d. PROJECT NUMBER	
		5e. TASK NUMBER	
		5f. WORK UNIT NUMBER	
7. PERFORMING ORGANIZATION NAME(S) AND ADDRESS(ES) **Department of Electrical Engineering, University of South Carolina, Columbia, SC 29208, USA**		8. PERFORMING ORGANIZATION REPORT NUMBER	
9. SPONSORING/MONITORING AGENCY NAME(S) AND ADDRESS(ES)		10. SPONSOR/MONITOR'S ACRONYM(S)	
		11. SPONSOR/MONITOR'S REPORT NUMBER(S)	
12. DISTRIBUTION/AVAILABILITY STATEMENT **Approved for public release, distribution unlimited**			
13. SUPPLEMENTARY NOTES **See also ADM001789, Fuel Cell Technology Hybrid Advanced Fuel Cell Power Sources., The original document contains color images.**			
14. ABSTRACT			
15. SUBJECT TERMS			

16. SECURITY CLASSIFICATION OF:			17. LIMITATION OF ABSTRACT	18. NUMBER OF PAGES	19a. NAME OF RESPONSIBLE PERSON
a. REPORT **unclassified**	b. ABSTRACT **unclassified**	c. THIS PAGE **unclassified**	**UU**	**33**	

Abstract

A study of the effects of cell temperature and pressure on anode polarization was achieved in this paper. A Langmuir and Temkin isotherm was used to study the CO adsorption equilibrium and the Heyrowski-Volmer mechanism for H_2 oxidation on a Pt/Ru-C catalyst. The anode overpotential curves were separated into four regions so that the adsorption rate constant for H_2 on Pt/Ru-C alloy could be determined. This separation allowed for the generation of a CO isotherm and it provided Lagmuir parameters to describe the CO adsorption equilibrium as a function of temperature and pressure.

Introduction

Recently Murthy *et al.*[1] show dramatic changes is steady state performance of a PEMFC when the temperature was changed from 70°C to 90°C with 500 ppm CO in H_2 (CO/H_2). They also show substantial changes in the rates of poisoning and recovery for this 20°C temperature change. These data were obtained using a Pt/Ru-C alloy electrode. Also recently Springer *et al.*[2] showed equations to study both steady and transient coverage of CO on membrane and electrode assemblies (MEA) with platinum catalysts. These equations depend on a large number of thermodynamic and kinetic parameters for adsorption and electrochemical oxidation of both hydrogen and CO. They gave a set of parameters that fit their data and with these parameters and their equations they were able to obtain agreement with steady state voltage-current data as a function of CO concentration and system pressure. However they did not investigate the effect of temperature and how these parameters differ for an alloy, particularly Pt/Ru-C. Other studies have shown that there is a significant change in cell performance due to a change in temperature at low CO concentrations (i.e., 20 ppm)[3]. There have also been several studies showing the
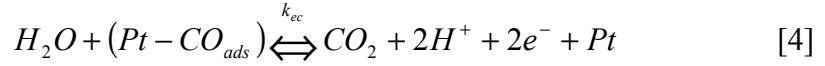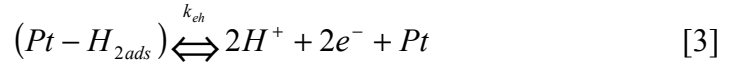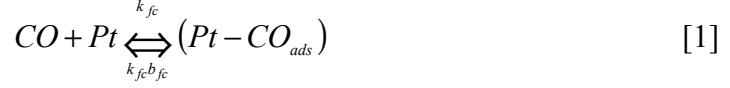
effect of an alloy, such as Pt/Ru-C on the overall poisoning effect of CO in the PEMF[3-7]. In this paper we focus on the change in these parameters as a function of temperature and pressure for both steady state and transient behavior during exposure to CO in H_2.

We are motivated by recent anodic polarization data that were reported for relatively high concentrations of CO/H_2 on a PRIMEA® MEA Series 55[1,8,9]. Current work in our laboratory is directed at the effect of temperature and pressure on the steady state and the rates of recovery and poisoning during exposure to concentrations of 500, 3000 and 10000 ppm CO/H_2. Specifically data were reported at 202 kPa for 70°C and 90°C in addition to the steady state results[1]. Rates of poisoning and recovery for step changes in the CO levels in hydrogen were also reported. Examples of these transient data are shown in Figure 1 where the cell was operated at a fixed current density of 600 mA/cm^2 with an initial stream of pure hydrogen. The decrease and increase in voltage resulted from changes in the CO concentration in the anode feed. We also have polarization curves for concentrations of 500 and 3000 CO/H_2 at 101 kPa and 70°C[8]. However since major emphasis was on providing poisoning and recovery rates rather than for studying the effect of cell temperature on cell performance, the framework provide for that work is limited and will be given a lower priority in estimating the parameters.

The objective of this study is to provide parameters for the equations that describe a Pt/Ru-C catalyst used in high performance MEA such as PRIMEA® MEA Series 55. These parameters will allow the description of performance as a function of temperature and pressure. The sensitivity of the predictions to changes in the parameters will also be presented.

Theory

Giorgi *et al.*[6] recently proposed the Heyrovski-Volmer mechanism for the oxidation of H_2 on a Pt/Ru-C catalyst. Thus a set of reactions for the alloy should be written:

$$CO + Pt \underset{k_{fc}b_{fc}}{\overset{k_{fc}}{\Longleftrightarrow}} \left(Pt - CO_{ads}\right) \tag{1}$$

$$H_2 + Pt \underset{k_{fc}b_{fh}}{\overset{k_{fh}}{\Longleftrightarrow}} \left(Pt - H_{2ads}\right) \tag{2}$$

$$\left(Pt - H_{2ads}\right) \overset{k_{eh}}{\Longleftrightarrow} 2H^+ + 2e^- + Pt \tag{3}$$

$$H_2O + \left(Pt - CO_{ads}\right) \overset{k_{ec}}{\Longleftrightarrow} CO_2 + 2H^+ + 2e^- + Pt \tag{4}$$

Then the rate expressions for the coverage of CO and H_2 on the Pt sites of the alloy can be written:

$$c_t \frac{d\theta_{CO}}{dt} = k_{fc}P_{CO}\left(1 - \theta_{CO} - \theta_H\right) - k_{fc}b_{fc}\theta_{CO} - \frac{i_{co}}{2F} \tag{5}$$

$$c_t \frac{d\theta_H}{dt} = k_{fh}P_{H_2}\left(1 - \theta_{CO} - \theta_H\right) - k_{fh}b_{fh}\theta_H - \frac{i_h}{2F} \tag{6}$$

Where:

$$i_{co} = i_{0,co}\left(\frac{\theta_{CO}}{\theta_{CO,eq}} e^{2f\eta_{aco}(1-\beta_{co})} - \frac{1-\theta_{CO}-\theta_H}{1-\theta_{CO,eq}-\theta_{H,eq}} e^{-2f\eta_{aco}\beta_{co}} \right) \tag{7}$$

$$i_h = i_{0,h}\left(\frac{\theta_H}{\theta_{H,eq}} e^{2f\eta_{ah}(1-\beta_h)} - \frac{1-\theta_{CO}-\theta_H}{1-\theta_{CO,eq}-\theta_{H,eq}} e^{-2f\eta_{ah}\beta_h} \right) \tag{8}$$

$$i_{0,co} = 2Fk_{ec}P_{H_2O}^{\beta_{co}}\theta_{CO,eq}^{\beta_{co}}P_{CO_2}^{1-\beta_{co}}\left(1 - \theta_{CO,eq} - \theta_{H,eq}\right)^{1-\beta_{co}} \tag{9}$$

$$i_{0,h} = 2Fk_{eh}\left(1 - \theta_{CO,eq} - \theta_{H,eq}\right)^{1-\beta_h}\theta_{H,eq}^{\beta_h} \tag{10}$$

$$\eta_{aco} = \frac{1}{2}\left(\eta_a - U_{CO}^\theta\right) \tag{11}$$

$$\eta_{ah} = \eta_a \qquad\qquad \text{for } i_{total} = i_h$$

$$= \frac{1}{2}\left(\eta_a + U_{CO}^{\theta}\right) \qquad\qquad \text{for } i_{total} = i_h + i_{co} \qquad [12]$$

This mechanism is in contrast to the Tafel-Volmer mechanism of H_2 oxidation on Pt used by Springer *et al.*[2]. Note that in Reaction 1-4 and Equations 5 and 6, we have followed the notation of Springer *et al.*[2] and thus one can recognize that the first and second terms in Equation 6 do not include a power 'n' which should be equal to 2 for the Tafel-Volmer mechanism. The molar area density of catalyst sites, c_t, has units of mol/cm^2. The adsorption rate constants k_{fc} and k_{fh} are for CO and H_2 adsorption respectively with units of mol/s-cm^2-atm. b_{fc} ($1/K_{eq,co}$) and b_{fh} ($1/K_{eq,h}$) represent the back-to-forward CO and H_2 adsorption ratio with Pa units. Also k_{ec} and k_{eh} are the electrochemical oxidation rate constants for CO and H_2 oxidation respectively, with units of mol/cm^2-s.

Equations 7 and 8 are the current density expressions for CO and H_2 as a function of their respective overpotentials and coverage and Equations 9 and 10 are their respective exchange current density expressed in terms for there respective equilibrium coverage. Equations 11 and 12 are the overpotentials of CO and H_2 in terms of the experimental anode overpotential assuming that the equilibrium potential for H_2 oxidation is zero and that the anode overpotential for H_2 oxidation in the absence of CO is negligible. At the exchange current density, therefore in absence of H_2 and CO oxidation (i.e., at $i_{total} = 0$) the following expressions can be derived for the steady state equilibrium θ_{CO} and θ_H:

$$\theta_{CO,eq} = \frac{1}{1 + \dfrac{b_{fc}}{P_{CO}}\left(1 + \dfrac{P_{H_2}}{b_{fh}}\right)} \qquad \theta_{H,eq} = \frac{1}{1 + \dfrac{b_{fh}}{P_{H_2}}\left(1 + \dfrac{P_{CO}}{b_{fc}}\right)} \qquad [13]$$

Note that these are their equilibrium coverage. The sum of the individual current densities, i_h and i_{co}, is the total or system current.

CO Isotherm Models

The two most referred to models for CO adsorption onto Pt in a Pt-C or Pt alloy catalysis are the Langmuir and Temkin isotherms. If we take Equation 13 in the absence of H_2 we get the well known Langmuir model, shown below.

$$\theta_{CO,pure} = \frac{1}{\dfrac{b_{fc}}{P_{CO}} + 1}$$

[14]

Taking the relationship presented by Chafik *et al.*[13] between the equilibrium adsorption coefficient ($K_{eq} = 1/b_{fc}$) and the adsorption energy, b_{fc} is defined as the following:

$$b_{fc} = \frac{1}{A} \exp\left[\frac{-E_{ads}}{RT}\right]$$

[15]

Where A is the pre-exponential term in their expression and E_{ads} is the adsorption energy. Note that as in the work by Chafik *et al.*[13], A was determined at a fixed temperature (600 K). A Langmuir isotherm model assumes that E_{ads} is constant with θ_{CO}. Therefore Equation 15 can be used as it is for a single value of E_{ads}. However in the case of Temkin isotherm it is assumed that E_{ads} changes linearly with θ_{CO} according to the following expression:

$$E_{ads} = E_0 (1 - \alpha\theta_{CO,pure})$$

[14]

Where E_0 is E_{ads} at $\theta_{CO} = 0$ and α is the fitting parameter that is independent of temperature. If we take ΔE to be the difference between E_{ads} at $\theta_{CO} = 0$ and at $\theta_{CO} = 1$ then from Equation 14 we get $\Delta E = \alpha E_0$. Upon substitution into Equation 15 the following expression for b_{fc} as a function of θ_{CO} is obtained:

6

$$b_{fc} = b_{fc0} \exp\left[\frac{\delta(\Delta G_{CO})}{RT}\theta_{CO,pure}\right] \qquad [15]$$

$$b_{fc0} = \frac{1}{A}\exp\left[\frac{-\Delta G_{CO}\big|_{\theta_{CO}=0}}{RT}\right] \qquad [16]$$

Note that this expression is similar to that given by Springer et al.[2] Where ΔE is $\delta\Delta G_{CO}$ in notation used by Springer et al.[2]. Also note that b_{fc0} depends on temperatures, which was fixed in the work by Springer et al.[2].

Rate of Poisoning and Recovery

All poisoning and recovery experiments in Ref. 1 and 8 where conducted at a fixed current and their results expressed as cell voltage as a function of time. Hence taking the derivative of the sum of the two current densities (Equation 7 and 8) and equating them to zero, the following expression can be derived for change in the anode overpotential:

$$\frac{d\eta_a}{dt} = -\frac{\gamma_3\dfrac{d\theta_H}{dt} + \gamma_4\dfrac{d\theta_{CO}}{dt}}{\gamma_1 + \gamma_2} \quad \text{for } i_{total} = i_h + i_{co}$$

$$= -2\frac{\gamma_3\dfrac{d\theta_H}{dt} + \gamma_4\dfrac{d\theta_{CO}}{dt}}{\gamma_1} \quad \text{for } i_{total} = i_h \qquad [17]$$

Where:

$$\gamma_1 = 2f\left(i_{h,a} - \beta_h i_h\right) \qquad [18]$$

$$\gamma_2 = 2f\left(i_{co,a} - \beta_{co}i_{co}\right) \qquad [19]$$

$$\gamma_3 = \frac{\theta_{H,eq}}{\theta_H}i_{h,a} + \frac{1-\theta_{CO,eq}-\theta_{H,eq}}{1-\theta_{CO}-\theta_H}\left(i_{h,c} + i_{co,c}\right) \qquad [20]$$

$$\gamma_4 = \frac{\theta_{CO,eq}}{\theta_{CO}} i_{co,a} + \frac{1 - \theta_{CO,eq} - \theta_{H,eq}}{1 - \theta_{CO} - \theta_H} \left(i_{h,c} + i_{co,c} \right) \qquad [21]$$

For:

$$i_{h,a} = i_{0,h} \left(\frac{\theta_H}{\theta_{H,eq}} \right) e^{2 f \eta_{ah}(1-\beta_h)} \qquad\qquad i_{co,a} = i_{0,co} \left(\frac{\theta_{CO}}{\theta_{CO,eq}} \right) e^{2 f \eta_{aco}(1-\beta_{co})} \qquad [22]$$

$$i_{h,c} = i_{0,h} \left(\frac{1 - \theta_{CO} - \theta_H}{1 - \theta_{CO,eq} - \theta_{H,eq}} \right) e^{-2 f \eta_{ah}\beta_h} \quad i_{co,c} = i_{0,co} \left(\frac{1 - \theta_{CO} - \theta_H}{1 - \theta_{CO,eq} - \theta_{H,eq}} \right) e^{-2 f \eta_{aco}\beta_{co}} \quad [23]$$

Equation 17 gives an expression that supports the assumption that the poisoning and recovery rates are governed by surface coverage phenomena[1, 8].

The anode potential curves shown in Ref. 8 were determined by subtracting the cell voltage in the presence of CO from that of neat H_2 at a fixed current. This was done with the assumption that the mass transfer controlled ovepotential from O_2 diffusion is only a function of current and that the anode overpotential from H_2 oxidation during neat H_2 is negligible. The expression below describes the anode overpotential following the above assumptions:

$$\eta_a(t) = V_{cell}\big|_{H_2(CE)} - V_{cell}\big|_{CO/H_2}(t) \qquad [24]$$

Where $V_{cell}\big|_{H_2(CE)}$ is the cell voltage for neat hydrogen at a particular current density on clean electrode (CE). Note that its value does not change because they depend on current, which is fixed during the experiment. Therefore the change is brought about by the anode polarization, which depends on the rate of coverage of H_2 and CO.

After some poisoning experiments, Murthy *et al.*[1,8] observed that the cell did not recover to its original value and thus we write $V_{cell}\big|_{CO/H_2} = V_{cell}\big|_{H_2(PE)}$. Where $V_{cell}\big|_{H_2(PE)}$ corresponds to the cell voltage for neat hydrogen on a poisoned electrode (PE). We speculate that some sites were non-recoverable from exposure to CO and thus additional polarization can be written:

8

$$\eta_a\big|_{H_2(PE)} = V_{cell}\big|_{H_2(CE)} - V_{cell}\big|_{H_2(PE)} \qquad [25]$$

That is, $\eta_a\big|_{H_2(PE)}$ is the anode overpotential resulting from the H$_2$ oxidation reaction for an

exposed electrode. This value changes depending on the degree of CO poisoning.

Results and Discussions

These equations depend on the twelve parameters; b_{fc} ($\delta(\Delta G_{CO})$, $\Delta G_{CO}\big|_{\theta_{CO}=0}$, A) b_{fh}, k_{fc},

k_{fh}, k_{ec}, k_{eh}, β_h, β_{co}, $U_{CO}{}^{\theta}$ and c_t. Eleven of parameters were estimated using the steady state data

from and the remaining from transient data from Ref. 1. To estimate the values of these eleven

parameters each steady state anode overpotential performance curves was separated into four

distinct regions shown in Figure 2. The data in Figure 2 is for 3000 ppm CO in H$_2$ at 70°C and

202 kPa from Ref. 1. The sequence for these estimation performed on the data from Ref. 1 for

the conditions listed in Table I is as follows: b_{fh} and k_{eh} are obtained from Region I; $\delta(\Delta G_{CO})$,

$\Delta G_{CO}\big|_{\theta_{CO}=0}$ and k_{fh} are obtained next from Region II; finally k_{fc}, k_{ec} and β_{co} are obtained from

Region III. For three of the four remaining points A, $U_{CO}{}^{\theta}$ and β_h their values are assumed in a

manner consistent with the data of Ref 1. Finally c_t is obtained from the transient recovery and

poisoning.

The objective function show below was used in estimating the parameters described in

detail below:

$$OF = \sum_{C=1}^{N_C}\sum_{P=1}^{N_P}\sum_{T=1}^{N_T}\sum_{D=1}^{N_D}\left(\eta_a{}^{obs} - \eta_a{}^{pred}\right)^2_{D,T,C} \qquad [26]$$

Where P, C, T and D are the CO concentrations, cell Pressure, cell temperature and data range

respectively.

Estimating b_{fh} and k_{eh}: Region I (Low Polarization Region)

The anode overpotential in Region I shown in Figure 2 is quite low. Which indicates that the H_2 oxidation reaction has enough available free surface for the reaction even after many sites have been covered with CO[2, 5]. In this region we assume that the coverage of CO remains at equilibrium throughout Region I and that i is linear with η_a at low current density values. Inherent in that assumption is fact that θ_H has to be a low enough for θ_{CO} to remain at its equilibrium value even after a potential is applied. Also this will indicates that θ_H is also low in the absence of any competing adsorbent. Therefore a value of 2% was assumed for θ_H^* which is the equilibrium H_2 coverage in the absence of CO. Then considering only the steady adsorption of H_2 without the presence of CO, from Equation 11, a relationship of the following can be formed for b_{fh}:

$$\frac{b_{fh}}{P_{H_2}} = \frac{\left(1 - \theta_H^*\right)}{\theta_H^*} \qquad [27]$$

The ratio b_{fh}/P_{H2} =10 for the assumed value of θ_H^*. We determined b_{fh} based on that P_{H2} at 202 kPa since for which more data was available. Note that b_{fh} was considered to be constant with temperature since there was no significant difference in cell performance under neat H_2 operation at 70 and 90°C.

Next we determined k_{eh} using the value of b_{fh} determined from above. The data corresponding to the condition of 500 ppm CO/H_2 at 90°C shown in Table II was used in determining k_{eh}. Assuming that i_h is linear with η_a and that $\theta_H = \theta_{H,eq}$ throughout Region I, the linear form of Equation 20 shown below was used.

$$i_h = i_{0,h} \left(\frac{\theta_H}{\theta_{H,eq}} - \frac{1 - \theta_{CO} - \theta_H}{1 - \theta_{CO,eq} - \theta_{H,eq}} \right. $$
$$\left. -2f \left[\frac{\theta_H}{\theta_{H,eq}} - \beta_h \left(\frac{\theta_H}{\theta_{H,eq}} - \frac{1 - \theta_{CO} - \theta_H}{1 - \theta_{CO,eq} - \theta_{H,eq}} \right) \right] \eta_{ah} \right) \quad [28]$$

The value of $i_{0,h}$ was varied such that a minimum OF was obtained and from which k_{eh} was then

determined using Equation 10.

Estimating b_{fc}: Region II (steady state total rate limited by available surface)

In this region the sites covered by the adsorbed CO limit the H_2 oxidation reaction hence

the sharp increase in the anode overpotential. At this point, the available free sites for the

oxidation reaction are used and the H_2 surface coverage approaches zero. We then use i_{total} equal

to a surface limited current density, $i_{l,\theta CO}$. When this occurs, the anodic polarization continues to

increase without bound until the adsorbed CO is removed from the surface by oxidation.

Therefore θ_{CO} is constant up from $\eta_a = 0$ until an overpotential corresponding to $i_{l,\theta CO}$. Applying

these limitations to the steady adsorption forms of Equations 5 and 6 including electrooxidation

of H_2 and solving those systems of equations for θ_{CO} and θ_H yeilds:

$$\frac{i_{l,\theta_{co}}}{2F} = k_{fh} P_{H_2} \left(\frac{b_{fc}}{b_{fc} + P_{CO}} \right) \quad [26]$$

Where $i_{l,\theta CO}$ is the total rate fixed by the non-oxidized CO on the surface of the electrode. Notice

that the above expression is similar to that given by Springer *et al.*[2] however the exponent 'n'

does not appear on the bracketed expression due to the previously mentioned assumption for H_2

the oxidation reaction on Pt/Ru-C.

Values of $i_{l,\theta CO}$ were determined at the point of inflection of the anode overpotential

curves (i.e. $i = i_{l,\theta CO}$ at $d^2\eta_a/di^2 = 0$) in Region II for all the conditions studied except for 500 ppm

CO/H$_2$ at 90°C and shown in Table 2. The steady state form of Equations 5 and 6 along with Equation 8 above for i$_{total}$ = i$_h$ where solved simultaneously for θ$_{CO}$, θ$_H$, and η$_a$ with these values of i$_{l,θCO}$ for various values of b$_{fc}$ and k$_{fh}$ such that a minimum OF was determined in Region II. The values determined for k$_{fh}$ will be discussed in detail in a following section. With these values of b$_{fc}$, θ$_{CO,eq}$ was determined using Equation 11 and plotted versus b$_{fc}$ shown in Figure #. The Temkin parameters, δ(ΔG$_{CO}$), $\Delta G_{CO}\big|_{\theta_{co}=0}$, from Equations 15 and 16, can now be determined from a best fit to the b$_{fc}$, θ$_{CO,eq}$ plot shown in Figure #.

Estimating k_{fc}, k_{ec}, and β_{co}: Region III (CO oxidation)

In Region III as shown on Figure 2, the slope of the polarization curve has decreased substantially. This indicates that there is now available surface for the H$_2$ oxidation reaction to occur normally. Also in this region i_h contributes most to the total rate[2,5] (i_h + i_{co}) because the flux of CO (i.e. i_{co}) is small due to the relative concentration of CO in the feed. Note that θ_{CO} approaches zero. Even though the CO oxidation reaction may not contribute significantly to the total rate, θ_{CO} decreases significantly from this reaction.

The smaller the value of k$_{fc}$ the more H$_2$ adsorption controls Region IV i.e. the value of k$_{fc}$ must be chosen such that i$_{co}$ approaches zero in that region (see Region IV below). Therefore a criteria of 100 μA/cm^2 as the maximum i$_{co}$ was assumed at the highest CO concentration (1% CO in H$_2$) for which k$_{fc}$ was determined. The steady state forms of Equations 5 and 6 and 7 and 8 along with i$_{total}$ = i$_{co}$+i$_h$, were solved simultaneously at a particular current density for the anode overpotential (η_a), θ_{CO} and θ_H assuming a value of 0.75 for β_{co} (α_{co} = 0.5) for various values of k$_{fc}$ and k$_{ec}$ until a minimum value of OF was obtained. However these values of k$_{fc}$ and k$_{ec}$ although optimized may generate i_{co} which depending on its size did not allow for the existence

of a Region IV as discussed above. Note that the values of k_{ec} and β_{co} used in determining k_{fc} are not optimized form the data however they were sufficient for that purposes of estimating k_{fc}.

Now with a value of k_{fc} known the same set of equations from above were again used for various values of k_{ec} and β_{co} until a minimum OF was obtained for all conditions except the ones at 500 and 3,000 ppm CO/H_2 at 101 kPa and 500 ppm CO/H_2 at 90°C and 202 kPa due to the lack of points in Region III.

Estimating k_{fh}: Region IV (H_2 adsorption limited)

A sharp increase in the overpotential similar to that observed in Region II can be seen from Figure 2 in this region. However the CO present on the surface has been fully oxidized ($\theta_{CO} = 0$) at this point meaning that there should be enough available surface to allow for the H_2 oxidation to proceed at the rate of hydrogen adsorption. Note that the intrinsic rate (i.e. per site) is dependent of c_t and that the total rate of hydrogen adsorption me be limited by the residual CO. unrestricted. That is some of the CO may permanently poison some of the sites. Now since the H_2 reaction becomes adsorption limited, the H_2 surface coverage approaches zero therefore fixing and i_{total} to $i_{l,p}$ reducing Equation 6 to:

$$\frac{i_{l,p}}{2F} = k_{fh}P_{H_2} \quad \text{at } i_{co} = 0 \qquad [27]$$

We determine $i_{l,p}$ from Equation 31 taking the values of k_{fh} determined from Region II. If these values are lower than the last current density value in the particual data being analyzed then b_{fc} will be re-estimated. All the values for $i_{l,\theta CO}$ and $i_{l,p}$ determined using the above analysis and used in the parameter estimation are shown in Table # below.

Anode Overpotential and CO Isotherm Comparisons

The anode overpotential η_a is determined by solving the steady state from of Equations 5 and 6 including the current expressions (Equations 7 and 8) with the parameters estimated according to the analysis shown above with values listed in Tables 1 and 2. Figure 3a and b show the reliability of the model and verifies the assumption pertaining to the H_2 oxidation reaction mechanisim. However since they were determined using the ilp values from the data, we are unable to see the effect of the isotherm.

In order to identify the best isotherm model for the given points on Figure 3 we start by comparing two well known Langmuir and Temkin isotherm models.

If this in fact was a Temkin isotherm, the value of ΔE will not change as the coverage changes. Therefore to check for this, the previously determined values of CO coverage in Table I were used solving Equation 28 for b_{fc}, and solving this and Equation 30 for ΔE. These values of ΔE shown in Table II are not constant for the data range studied which and change quite considerably especially for the 500 ppm CO/H_2 at 90°C data set. The same is true in the case of the Langumir model. Which indicate a different isotherm may be driving the process.

Figures 5a and b and 6a and b show a comparison in the anode overpotential predictions using the b_{fc} values from Table along with the $i_{l,p}$ values from Table I with those using the Langmuir model (Equation 28) for 70 and 90°C respectively. The predictions are not accurate in Region I where the anode overpotential is the lowest and is expected since the error in those points as a result of the method used in determining them in that region is usually pronounced. However they fit reasonably in the Regions II - IV, which indicates that model and the parameters used that were estimated in this study are adequate for capturing the phenomena.

Observe that the curves using the Langmuir model generally fit the curves close to those using Equation 27 at the higher partial pressures in Region II, which can be expected upon observation of Figure 4. However there is a large deviation at the lower partial pressures in that region especially for 500 ppm CO/H_2 at 70°C and is expected since the Langmir model was unable to predict that point on the isotherm graph (Figure 4). Also note the severe deviation in the predicted anode polarization in the case of 500 ppm CO/H2 at 90°C from that of the actual polarization. This may be because of internal air-bleeding which is a result of additional however non-faradic CO oxidation by the O_2 crossing over from the cathode side. All the predictions did not show significant differences for Regions III and IV and is expected since the permanent poison phenomena is well defined.

The anode overpotential curves for the 1 atm data sets 3,000 and 500 ppm CO/H_2 collected in Ref. 1 along with the model predictions using the parameters in Table 2 are shown in Figure #. The values of ilco were determined directly from the data using a previously mention analysis and ilp was determined based on the isotherm in Figure #. Upon observing Figure # of Ref. 1 we can see

Poisoning and Recovery Comparisons

Figures 8-9 show the predictions of the model using the parameters estimated in this work shown in Table 2. These figure used the E_{ads} associated with the actual CO coverage used in constructing Figure 3 and the permanent poisoning parameters according to Figure 6 since they gave the best predictions for the steady state anodic polarization curves. All the predictions seem to follow the general trend of each curve although however they seem to under predict and over estimate the cell voltage in some areas. This is mainly attributed to the fact that there are

some differences between the cell voltage from the steady state anode polarization curves and that determined during poisoning and recovery for most of the data set and not because of the parameters. It is important to note that final cell voltage values were different for each CO partial pressure investigated and did not vary in a predictable way for the various runs at the end of recovery. The predictions were unable to accurately predict these final cell voltage values. This may be because a fixed value was used for the total density of sites, which may be different for each run.

The volume of the humidity bottle used for the experiments in Ref. 8 was measured to be 750 ml. The flow rate into the bottle was calculated, based on the analysis presented by W-k Lee (21), to be 1.68 cm^3/sec at 70°C.

$$P_{CO} = P_{CO}\big|_{t=0} \exp\left(-\frac{\Delta t}{\tau_B}\right)$$ [##]

Therefore the maximum residence time is around 446 seconds considering that the full volume of the bottle is utilized. As can be seen from the graph 60% of this value (200 seconds) gave the best fit to the curve validating the assumption that the partial pressure of CO in the humidity bottle can be acts as a time dependent CSTR and that the humidity bottle is where the gas spends the most time.

Conclusions

The Heyrovsky-Volmer mechanism was shown to be applicable for H$_2$ oxidation on a Pt/Ru-C catalyst. A Langmuir model was adequate for capturing the CO coverage for the range of partial pressure and temperatures studied particularly at higher partial pressures, which is typical of this type of isotherm. Region IV played an important role in the parameter estimation process as it revealed the effect of permanent poisoning of the overall adsorption rate constant

for H_2 adsorption necessary for predicting the limiting currents observed during CO oxidation. The sensitivity of the model to the isotherm validates that the adsorption and oxidation process of H_2 and CO are enough to capture the effect of CO poisoning in a PEMFC. The poisoning and recovery process could be modeled according to the development in the text with these parameters.

Acknowledgments

CARBEL, GORE-SELECT, PRIMEA, and GORE and designs are trademarks of W. L. Gore & Associates, Inc.

References

1. M. Murthy, M. Esayian, A. Hobson, W.-k. Lee, and J. W. Van Zee, *Journal of the Electrochemical Society* **150**, pp. A29-A34 (2003).

2. T. E. Springer, T. Rockward, T. A. Zawodzinski, and S. Gottesfeld, *Journal of the Electrochemical Society* **148,** A11-A23 (2001).

3. S. J. Lee, S. Mukerjee, E. A. Ticianelli, and J. McBreen, *Electrochemica Acta*, **44**, 3283-3293 (1999).

4. J. Divisek, H. F. Oetjen, V. Peinecke, V. M. Schmidt and U. Stimming, *Electrochimica Acta*, **43**, 3811-3815 (1998).

5. R. J. Bellows and E. Marucchi-Soos, in Proton Conducting Membrane Fuel Cells, S. Gottesfeld and T. F. Fuller, Editors, Proceedings Volume 98-27, p. 218, The Electrochemical Society Proceedings Series, Pennington, NJ (1999).

6. L. Giorgi, A. Pozio, C. Bracchini, R. Giorgi, and S. Turtu, *Journal of Applied Electrochemistry* 31, 325-334, (2001).

7. H. Igarashi, T. Fujino, and M. Watanabe, *Physical Chemistry Chemical Physics*, **3**, 306-314 (2001).

8. M. Murthy, M. Esayian, A. Hobson, S. MacKenzie, W.-k. Lee, and J. W. Van Zee, *Journal of the Electrochemical Society* **148**, pp. A1141-A1147 (2001).

9. M. Murthy, M. Esayian, A. Hobson, and S. MacKenzie, W-k. Lee and J. W. Van Zee, *Journal of New Materials for Electrochemical Systems*, To be published.

10. W.-k. Lee, J. W. Van Zee, and M. Murthy, *Fuel Cells*, 3, No. 1-2, 52-58, (2003)

11. J. Newman, *Electrochemical Systems*, p. 197, Prentice Hall, Inc., Englewood Cliffs, NJ (1973).

12. W. Vogel, J. Lundquist, P. Ross, and P. Stonehart, *Electrochimica Acta*, **20**, 79 (1975).

13. W-k. Lee, M. Murthy, and J. W. Van Zee, AICHE Presentation 86h, Spring 2002, New Orleans.

14. T. Chafik, O. Dulaurent, J. L. Gass, and D. Bianchi, *Journal of Catalysis*, **179**, 503-514 (1998).

15. R. I. Masel, *Principles of Adsorption and Reaction on Solid Surfaces*, p. 250-252, Interscience, New York (1996).

16. A. W. Adamson, *Physical Chemistry of Surfaces*, p. 626, Interscience, New York (1967).

17. W-k. Lee, Ph.D. dissertation, Department of Chemical Engineering, University of South Carolina, Columbia, SC (2000).
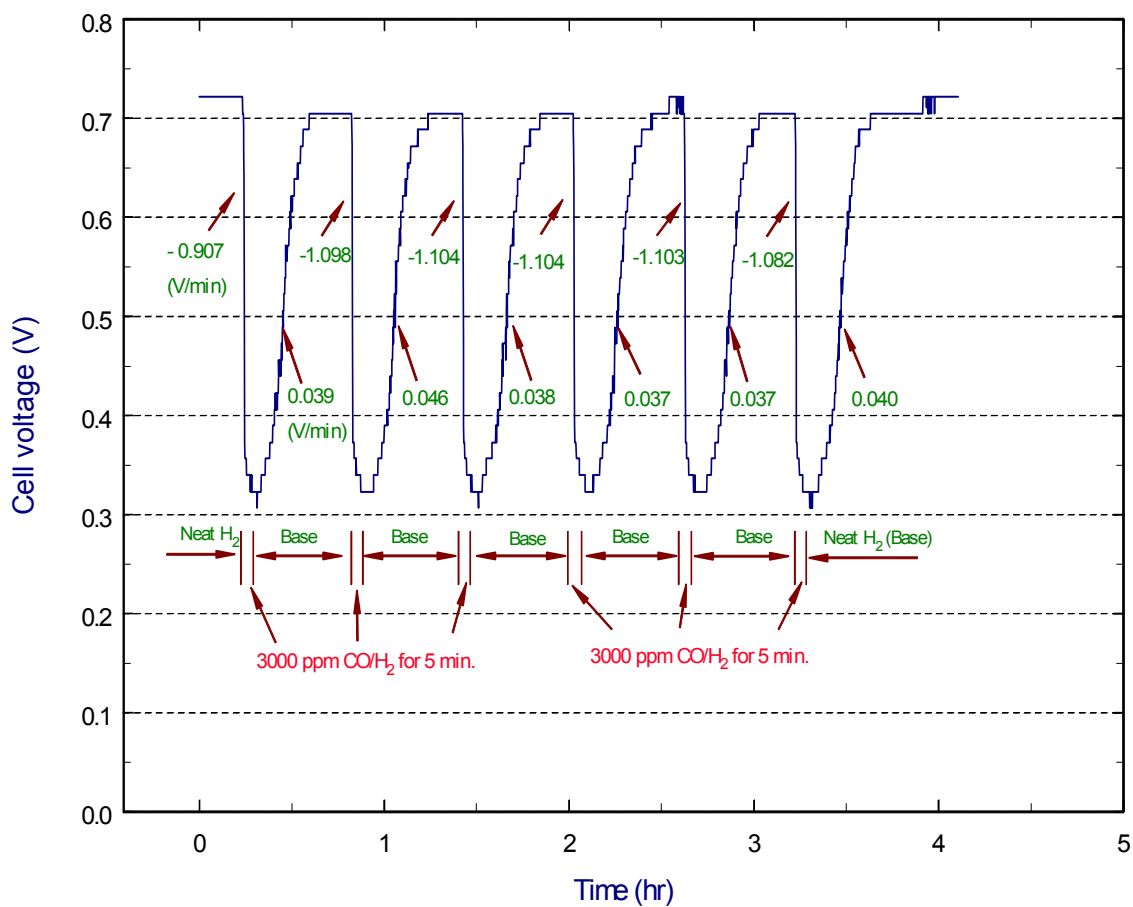
Figure 1. Transient performance with neat hydrogen and 3000 ppm CO at 600 mA/cm^2 with CARBEL^{TM} CL GDM. (T_{cell} = 70°C and P(A/C) = 15/15 psig)
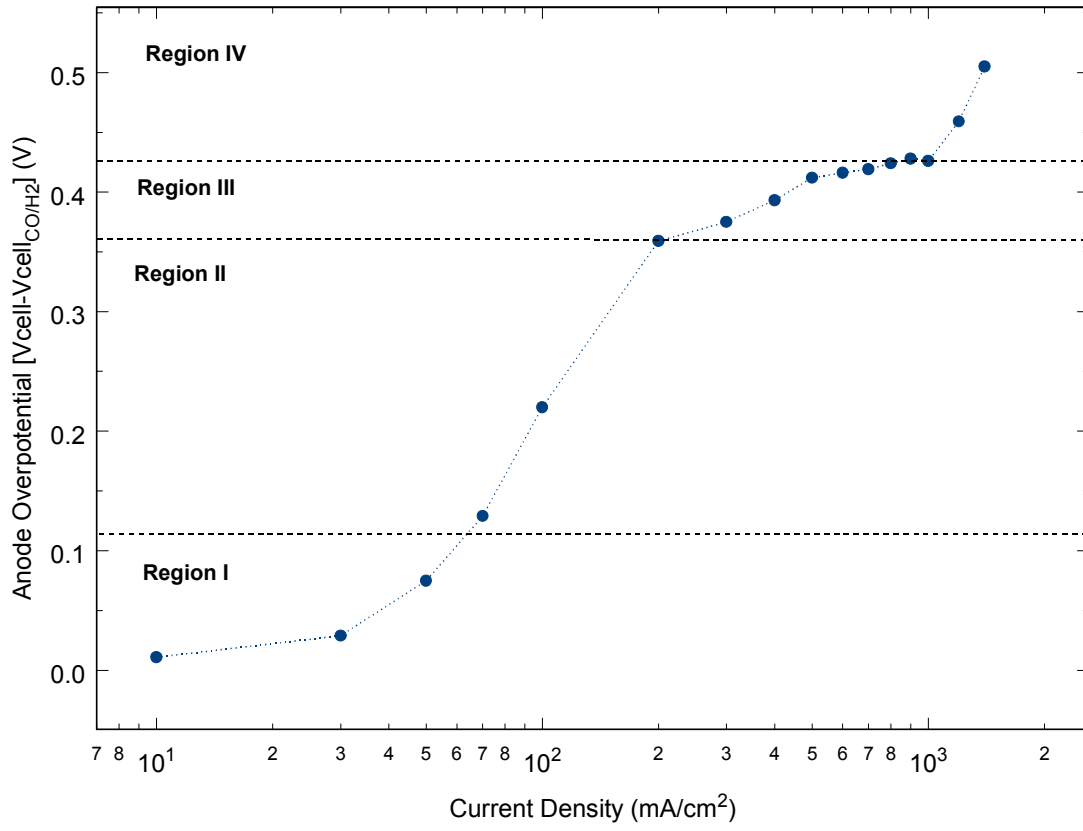
Figure 2. Regions identification graph (Data from Figure 3 of Ref. 1 for 3000 ppm CO in H_2 at 70°C and 202 kPa).
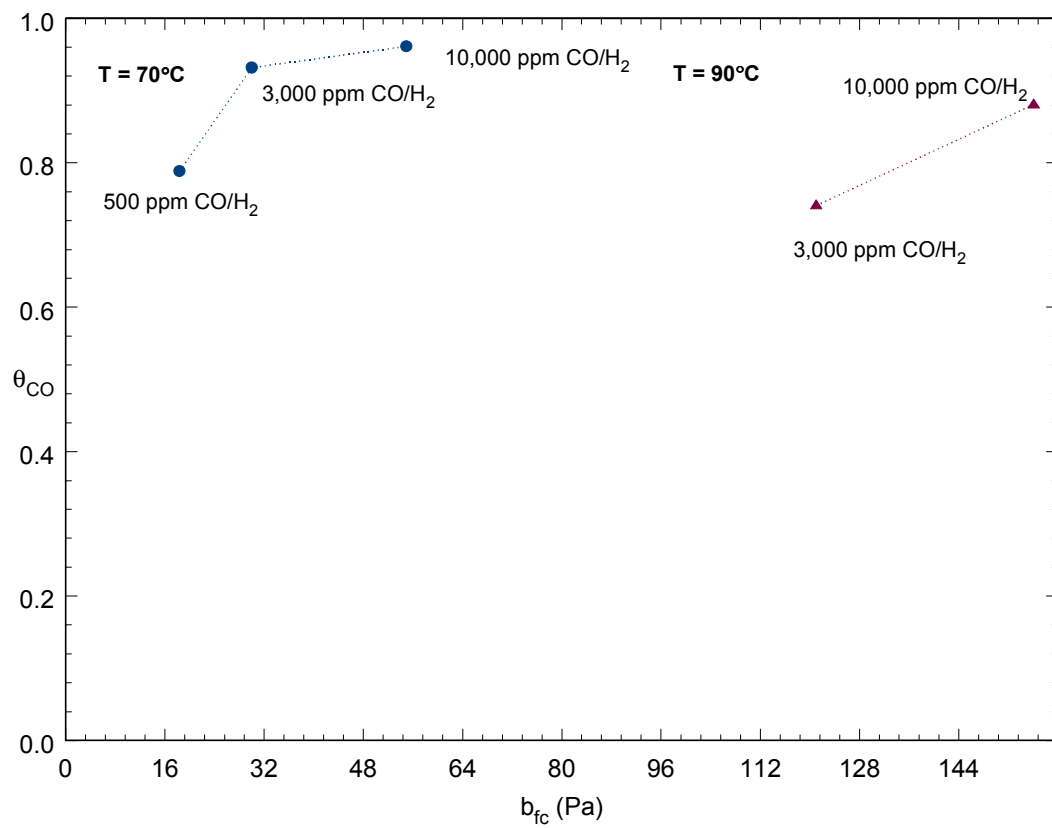
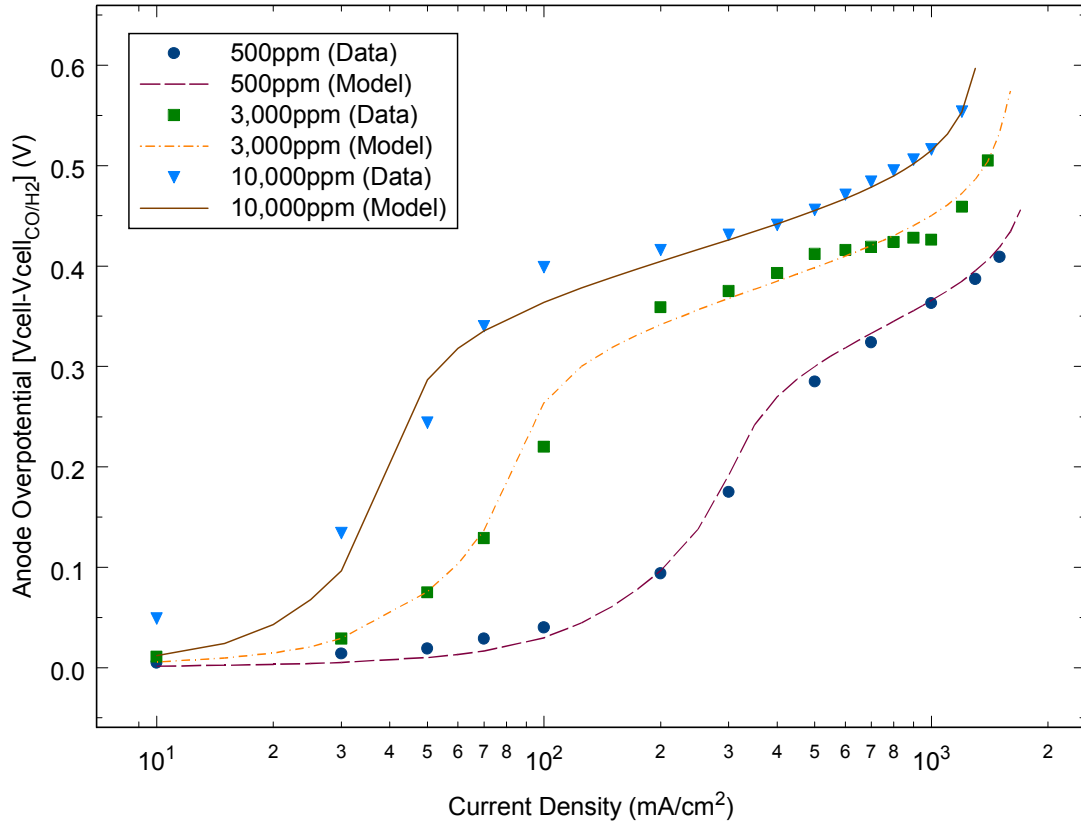Figure 10. b_{fc} versus θ_{CO} for 500, 3,000 and 10,000ppm of H_2/CO feed at 70 and 90°C

Figure 3a. Overpotential model comparison for ($\triangle$) 500, ($\blacksquare$) 3,000 and ($\bullet$) 10,000 ppm

H_2/CO at a cell temperature of 70°C (Lines are computed from Equations 5-8 using b_{fc} from
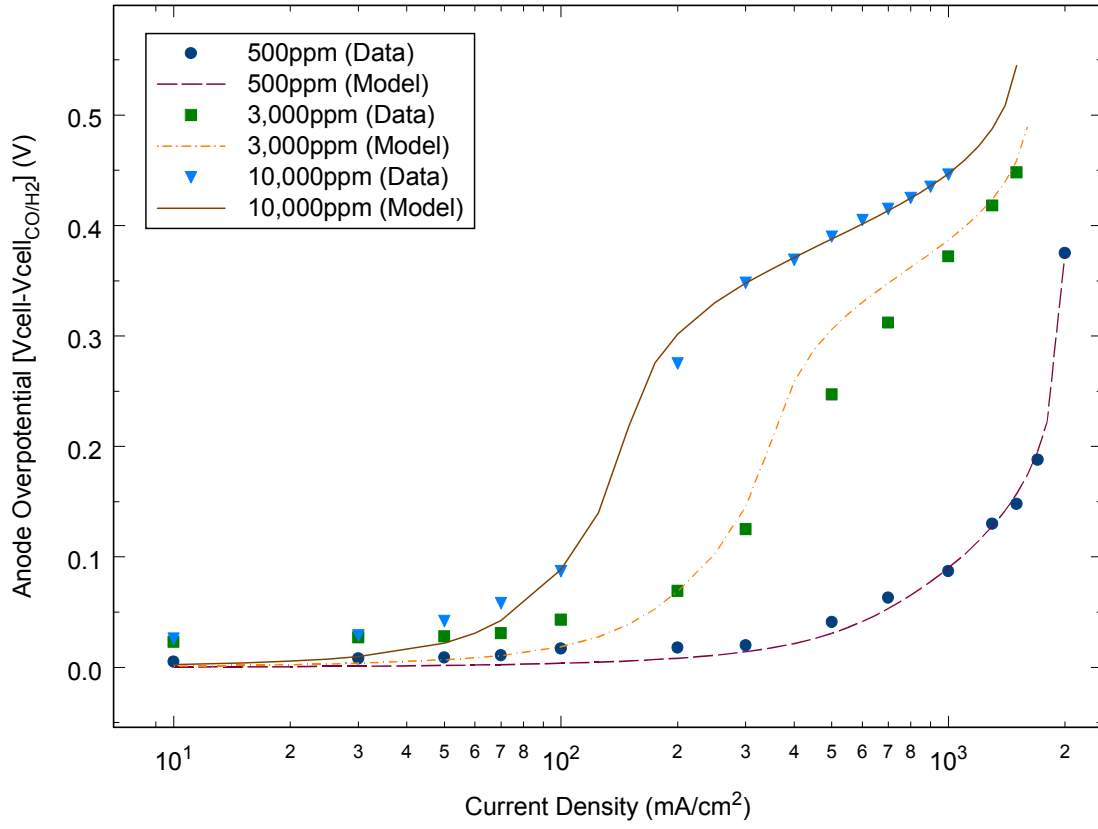
Table I and parameters from Table III).

Figure 3b. Overpotential model comparison for (▲) 500, (■) 3,000 and (●) 10,000 ppm H$_2$/CO at a cell temperature of 90°C (Lines are computed from Equations 5-8 using b_{fc} from Table I and parameters from Table III).
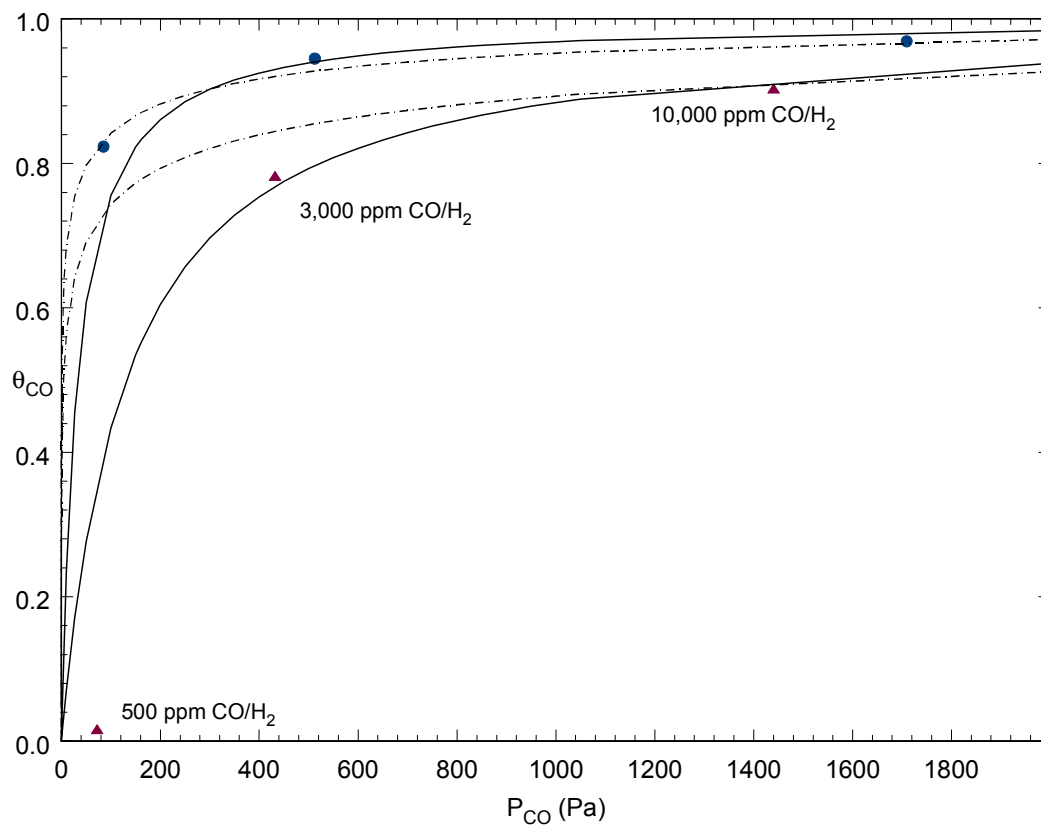
Figure 4. CO Isotherm comparison graph for CO for 500, 3,000 and 10,000ppm of H_2/CO feed at (●) 70 and (▲) 90°C (Temkin model (dashed line) and Langmuir model (line)).
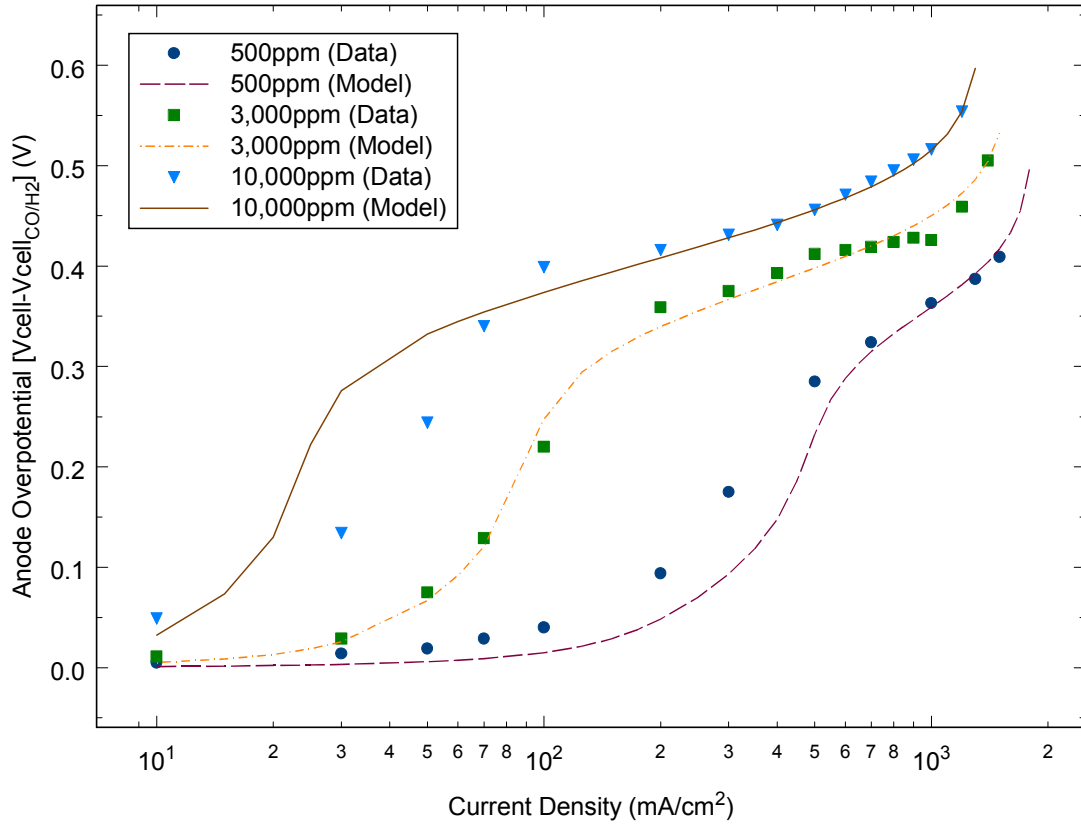
Figure 5a. Overpotential model comparison for (▲) 500, (■) 3,000 and (●) 10,000 ppm

H_2/CO at a cell temperature of 70°C (Lines are computed from Equations 5-8 using Lamgmuir

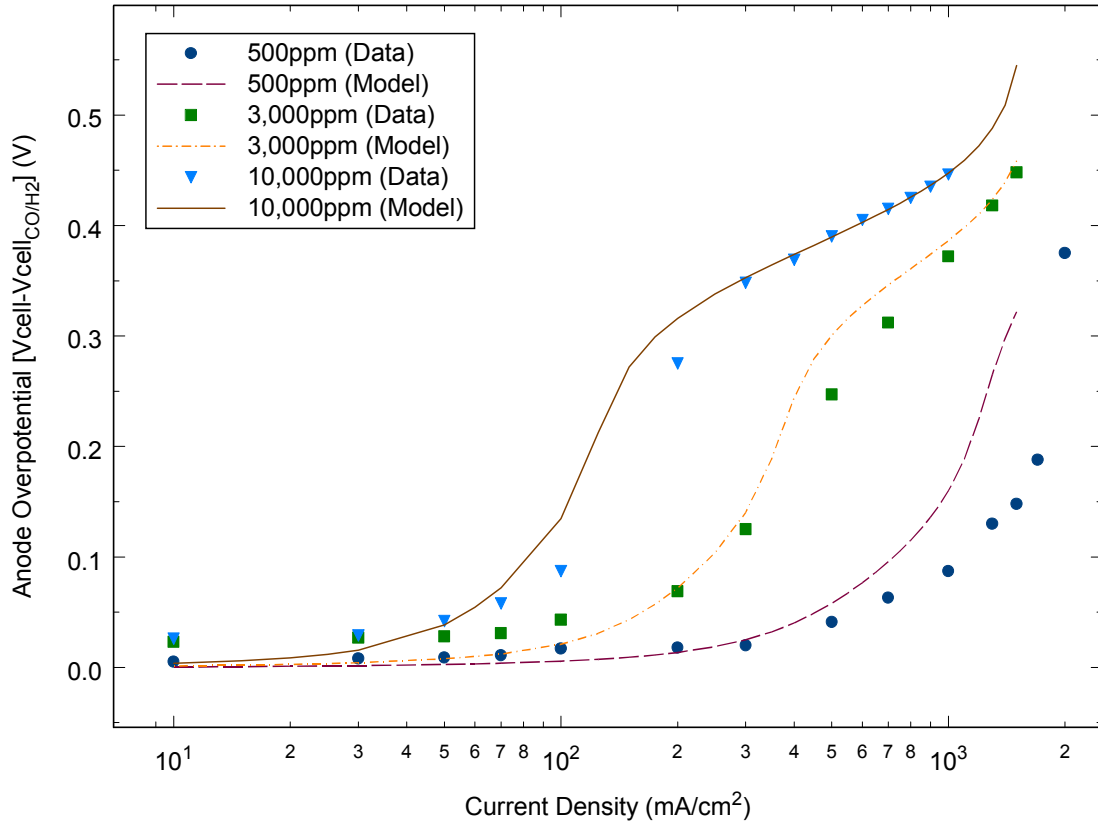Model i.e. b_{fc} from Equation 12 and parameters from Table III).

Figure 5b. Overpotential model comparison for (▲) 500, (■) 3,000 and (●) 10,000 ppm H_2/CO at a cell temperature of 90^oC (Lines are computed from Equations 5-8 using Lamgmuir Model i.e. b_{fc} from Equation 12 and parameters from Table III).

Figure 5a. Overpotential model comparison for ($\blacktriangle$) 500, ($\blacksquare$) 3,000 and ($\bullet$) 10,000 ppm H$_2$/CO at a cell temperature of 70°C (Lines are computed from Equations 5-8 using Temkin Model i.e. b_{fc} from Equation 14 and parameters from Table III).

Figure 5b. Overpotential model comparison for ($\triangle$) 500, ($\blacksquare$) 3,000 and ($\bullet$) 10,000 ppm H$_2$/CO at a cell temperature of 90°C (Lines are computed from Equations 5-8 using Temkin Model i.e. b_{fc} from Equation 14 and parameters from Table III).
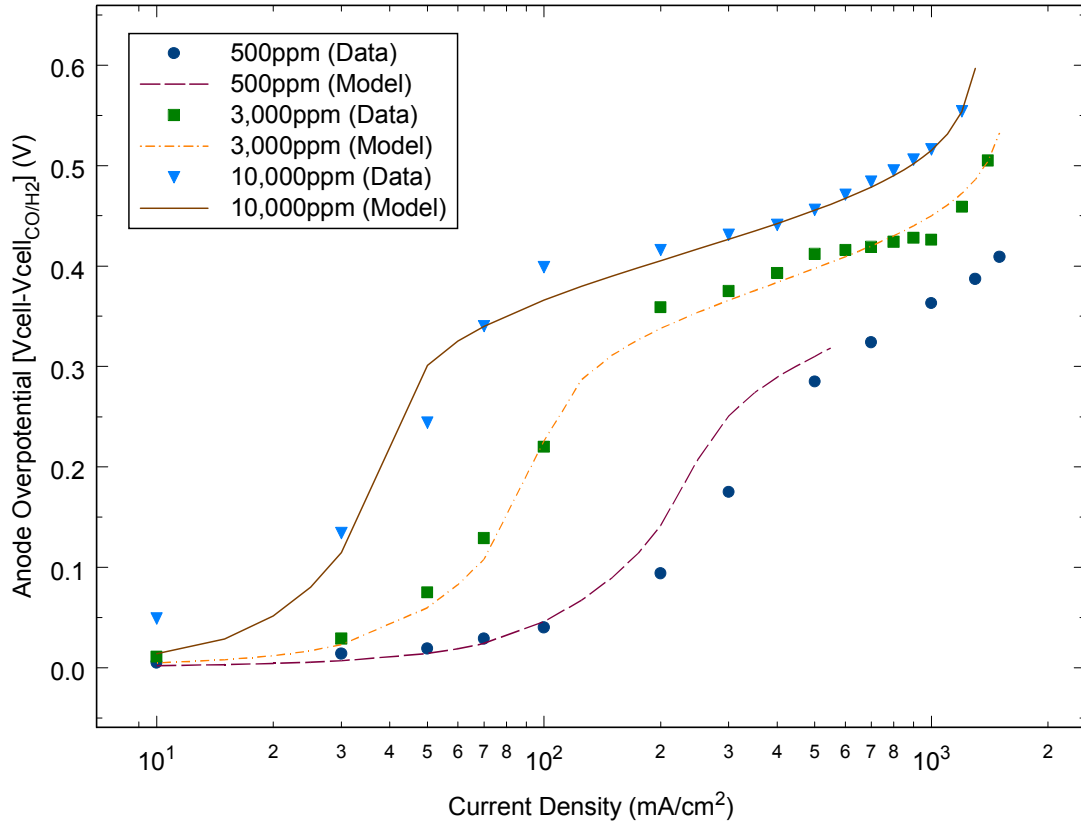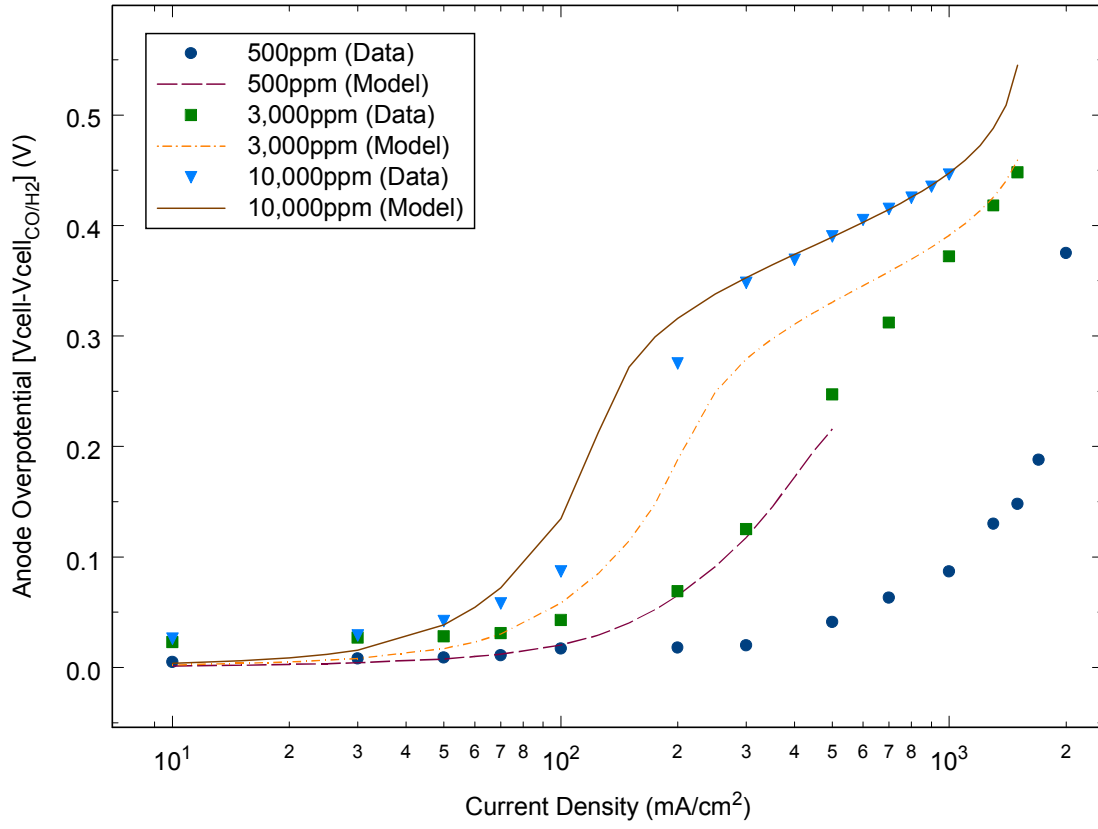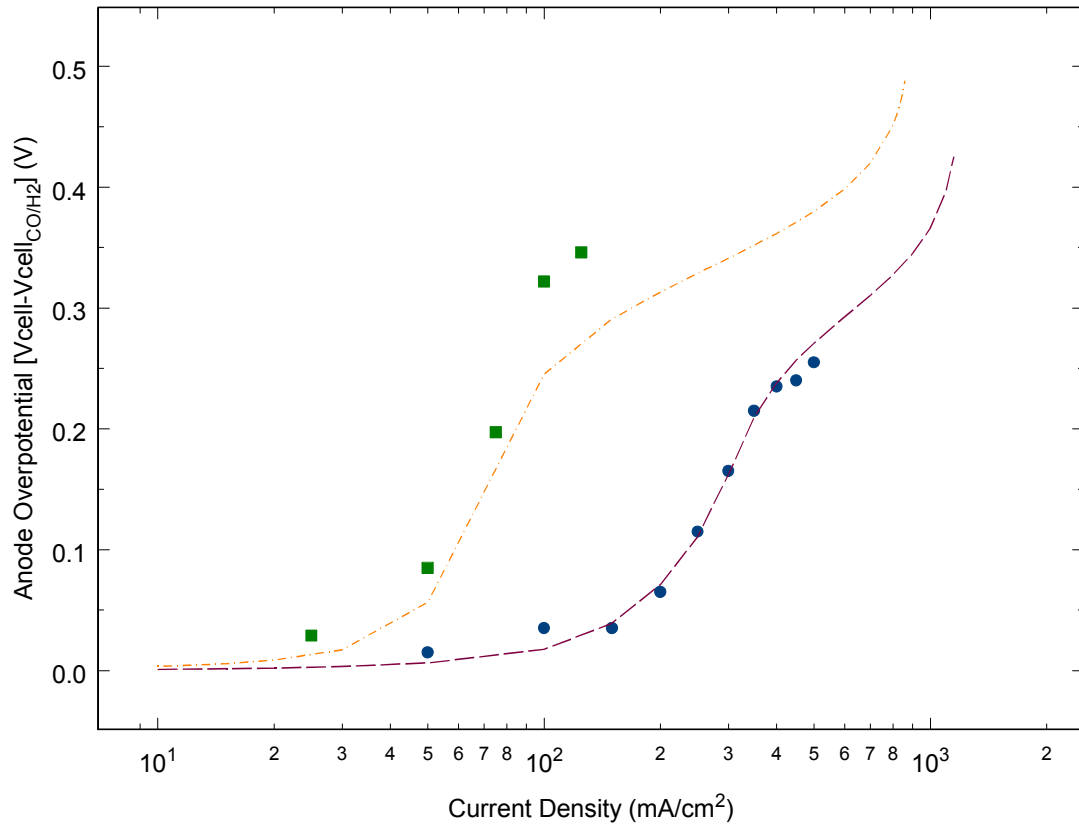
Figure 6a. Overpotential model comparison for (▲) 500 and (■) 3,000 ppm H_2/CO at a cell temperature of 70°C (Lines are computed from Equations 5-8 using b_{fc} from Table I and parameters from Table III).

Table 1. Summary of Data Used for Regional Analysis

Temperature (^{o}C)	Pressure (kPa)	CO Concentrations (ppm CO/H$_2$)
70	101	500
70	101	3,000
70	202	500
70	202	3,000
70	202	10,000
90	202	500
90	202	3,000
90	202	10,000

Table 2. Summary of Parameters Determined from Regional Analysis

<u>Parameters</u>
Region I: b_{fh}, k_{eh}
Region II: b_{fc} ($\delta(\Delta G_{CO})$, $\Delta G_{CO}\big|_{\theta_{co}=0}$, A)
Region III: k_{fc}, k_{eh}, β_{co}
Region IV: k_{fh}

Table 1. Value of $i_{l,p}$, $i_{l,\theta co}$ and b_{fc} determined from data

CO Concentration (ppm)	Temp (C)	P_{CO} (Pa)	$i_{l,p}$ (A/cm^2)	$i_{l,\theta CO}$ (A/cm^2)	b_{fc}/P_{CO}
500	70	85.5	2	0.328	0.196302
3,000	70	513	1.65	0.088	0.056836
10,000	70	1710	1.15	0.0399	0.035943

500	90	72	2.1	N/A	20
3,000	90	432	1.7	0.402	0.309509
10,000	90	1440	1.3	0.152	0.132504

Table 2. Comparison of CO Coverage from Data to Springer et al. values

CO Concentration (ppm)	Temp (C)	P_{CO} (Pa)	θ_{CO} (Nwoga)	θ_{CO} (Springer)	ΔE (J/mol)
500	70	85.5	0.835	0.994	879.7
3,000	70	513	0.946	0.999	2442.3
10,000	70	1710	0.965	0.999	4598.0
500	90	72	0.047	0.969	206819.3
3,000	90	432	0.763	0.994	3499.8
10,000	90	1440	0.883	0.998	4242.6

Table 3. List of Parameters Used in Model

b_{fh}/P_{H2}	4	k_{ec0}^{*}	$5.16 \times 10^{-5} \pm (5 \times 10^{-3})$ mol cm^{-2} s^{-1}
E_{ads}	$72.6 \pm (5 \times 10^{-3})$ kJ mol^{-1}	$E_{a,kec}$	60.8 kJ/mol
A	2.95×10^{-13} Pa^{-1}	β_h	0.75
k_{fc}	$0.2 \times 10^{-6} \pm (5 \times 10^{-3})$ mol cm^{-2} s^{-1} atm^{-1}	β_{co}	$0.6 \pm (5 \times 10^{-3})$
$k_{fh}^{c;eam}$	$7.34 \times 10^{-6} \pm (5 \times 10^{-3})$ mol cm^{-2} s^{-1} atm^{-1}		
k_{eh}	$1.3 \times 10^{-5} \pm (5 \times 10^{-3})$ mol cm^{-2} s^{-1}		

Figure Captions

Figure 1. Transient performance with neat hydrogen and 3,000 ppm CO at 600 mA/cm^2 with CARBEL$^{™}$ CL GDM. (T_{cell} = 70°C and P(A/C) = 15/15 psig).

Figure 2. Regions identification graph (Data from Figure 3 of Ref. 1 for 3000 ppm CO in H$_2$ at 70°C and 202 kPa).

Figure 3. CO Isotherm comparison graph for CO for 500, 3,000 and 10,000ppm of H_2/CO feed at (●) 70 and (▲) 90°C (The lines are computed from Equations 28 and 29 with the parameters in Table III).

Figure 4. Graph for values of $i_{l,p}/i_{l,p}^{clean}$ as a function of CO partial pressure at 70 and 90°C. Data points (■) and (●) are for 70 and 90°C respectively.

.

Figure 5a. Overpotential model comparison for (▲) 500, (■) 3,000 and (●) 10,000 ppm H_2/CO at a cell temperature of 70°C (Lines are computed from Equations 5-8 using b_{fc} from Table I and parameters from Table III).

Figure 5b. Overpotential model comparison for (▲) 500, (■) 3,000 and (●) 10,000 ppm H_2/CO at a cell temperature of 70°C (Lines are computed from Equations 5-8 using Lamgmuir Model i.e. b_{fc} from Equation 29 and parameters from Table III).

Figure 6a. Overpotential model comparison for (▲) 500, (■) 3,000 and (●) 10,000 ppm H_2/CO at a cell temperature of 90°C (Lines are computed from Equations 5-8 using b_{fc} from Table I and parameters from Table III).

Figure 6b. Overpotential model comparison for (▲) 500, (■) 3,000 and (●) 10,000 ppm H_2/CO at a cell temperature of 90°C (Lines are computed from Equations 5-8 using Lamgmuir Model i.e. b_{fc} from Equation 29 and parameters from Table III).